

Loss-Sensitive Generative Adversarial Networks on Lipschitz Densities

Guo-Jun Qi

Abstract—This paper presents a novel loss-sensitive generative adversarial net (LS-GAN). Compared with the classic GAN that uses a dyadic classification of real and generated samples to train the discriminator, we learn a loss function that can generate samples with the constraint that a real example should have a smaller loss than a generated sample. This results in a novel paradigm of loss-sensitive GAN (LS-GAN), as well as a conditional derivative that can generate samples satisfying specified conditions by properly defining a suitable loss function. The theoretical analysis shows that the LS-GAN can generate samples following the true data density we wish to estimate. In particular, we focus on a large family of Lipschitz densities for the underlying data distribution, allowing us to use a class of Lipschitz losses and generators to model the LS-GAN. This relaxes the assumption on the classic GANs that the model should have infinite modeling capacity to prove the similar theoretical guarantee. This provides a principled way to regularize a family of deep generative models with the proposed LS-GAN criterion, preventing them from being overfitted to duplicate few training examples. Furthermore, we derive a non-parametric solution that characterizes the upper and lower bounds of the losses learned by the LS-GAN. We conduct experiments to evaluate the proposed LS-GAN on classification and generation tasks, and demonstrate the competitive performances as compared with the other state-of-the-art models.

Index Terms—Loss-Sensitive GAN, Lipschitz density, image generation and classification

1 INTRODUCTION

Classic Generative Adversarial Net (GAN) [1] attempts to learn a discriminator and a generator simultaneously by playing two-player minimax game. Specifically, the discriminator aims to distinguish real samples from those generated by the generator, while the generator is learned by producing samples that can pass the check by the discriminator.

Take image synthesis as an example. On one hand, the discriminator seeks to learn the probability of a sample being a photo-realistic image. It treats natural images as positive examples, while the images produced by a paired generator as negative examples. On the other hand, the generator aims to produce images as photo-realistic as possible so that the discriminator would believe the generated images are real. A two-player's game is iteratively conducted at the discriminator's and the generator's interests.

However, a dyadic treatment of real and generated data as positive and negative examples may oversimplify the problem of learning a GAN model. Actually, as the generator improves, its generated samples would become more and more closer to the manifold of real samples; however, they are still being treated as negative examples to train the discriminator in the classic GAN. This could lead to an over-pessimistic discriminator characterizing the boundary between real and unreal samples. This would in turn limit the ability of learning a satisfactory generator that relies on an exact discriminator to capture the difference between real and unreal examples.

Moreover, from a theoretical perspective, the analysis behind the GAN makes a non-parametric assumption that the model has infinite modeling capacity [1] in order to

prove the density of generated samples equals the underlying data density we wish to estimate. This is a too strong assumption to hold: even a very deep network could not assume infinite modeling capacity to map any given input to an arbitrarily desired output. Even worse, a generative model with unlimited capacity would suffering from severe overfitting problem, and this is probably the reason for a collapsed generator that is stuck in producing the same data point since such a model would be powerful enough to aggressively push its generated samples close to the densest mode of the underlying density. The phenomenon has been observed in literature [2], [3], and a properly regularized learning objective is preferred to avoid the collapse while generating samples following the true density.

In this paper, we attempt to develop theory and models without such an assumption, which yields a novel Loss-Sensitive GAN (LS-GAN). Specifically, we introduce a loss function to quantify the quality of generated samples. Then a constraint is imposed to train the LS-GAN so that the loss of a real sample should be smaller than that of a generated counterpart by a unfixed Lipschitz-style margin that depends on how close they are to each other in a metric space. In this way, if a generated sample is already very close to a real example, the margin between their losses could vanish. This allows the model to focus on improving poor samples rather than wasting efforts on those samples that have already been well generated with satisfactory quality, thereby improving overall quality of generation results.

We also develop a new theory to analyze the proposed LS-GAN on Lipschitz densities. We argue that the reason of assuming “infinite modeling capacity” in the classic GAN is due to its ambitious goal to sample from an arbitrary data density without imposing any priors. However, the general principle in learning theory asserts “bias-free learning is futile,” which is known as no free lunch theorem in

• G.-J. Qi was with the Department of Computer Science, University of Central Florida, Orlando, FL, 32816.
E-mail: guojun.qi@ucf.edu

literature [4]. This prompts us to focus on a specific class of Lipschitz densities. This class of densities contain a large family of real-world data distributions, where the density of samples does not change abruptly when they are close to one another. We equip the Lipschitz densities with the distance metric that specifies the loss margin in the LS-GAN, and this allows us to show the resulting models can generate samples from the underlying data density even though they now have controlled rather than unlimited modeling capacity.

We further present a non-parametric solution to LS-GAN. It does not rely on any parameterized form of function, thereby exploring the whole space of Lipschitz functions for an optimal loss function. This non-parametric solution characterizes both the upper and lower bounds of the learned loss functions, which can shed some light on a principled approach to regularize the LS-GAN model to produce high-quality samples.

Moreover, we generalize the model to a Conditional LS-GAN (CLS-GAN) that can generate samples based on given conditions. Specifically, considering different classes as conditions, the learned loss function can be used as a classifier for supervised learning. The advantage of such a classifier lies in its intrinsic ability of exploring generated examples to reveal unseen variations for different classes. Experiment results also demonstrate competitive performance of the CLS-GAN classifier.

The remainder of this paper is organized as follows. Section 2 reviews the related work and summarizes our contributions. We will present the proposed LS-GAN in Section 3. In Section 4, we will analyze the LS-GAN, showing that its generated samples follow the underlying data density even with a class of Lipschitz losses and generators. We will discuss the algorithm details in Section 5, and show that the model can be generalized to take an input condition to generate data in Section 6. Experiment results are presented in Section 7, followed by the conclusion in Section 8.

2 RELATED WORK AND OUR CONTRIBUTIONS

It has been a long-term goal to enable synthesis of highly structured data such as images and videos.

Deep generative models, especially the Generative Adversarial Net (GAN) [1], have attracted many attentions recently due to their demonstrated abilities of generating real samples following the underlying data densities. In particular, the GAN attempts to learn a pair of discriminator and generator by playing a maximin game to seek an equilibrium, in which the discriminator is trained by distinguishing real samples from generated ones and the generator is optimized to produce samples that can fool the discriminator.

A family of GAN architectures have been proposed to implement this idea. For example, recent progresses [2], [3] have shown impressive performances on synthesizing photo-realistic images by constructing multiple strided and fractional-strided convolutional layers for discriminators and generators. On the contrary, [5] proposed to use a Laplacian pyramid to produce high-quality images by iteratively adding multiple layers of noises at different resolutions. [6]

presented to train a recurrent generative model by using adversarial training to unroll gradient-based optimizations to create high quality images.

In addition to designing different GAN networks, research efforts have been made to train the GAN by different criteria. For example, [7] presented an energy-based GAN by minimizing an energy function to learn an optimal discriminator, and an auto-encoder structured discriminator is presented to compute the energy. The authors also present a theoretical analysis by showing this variant of GAN can generate samples whose density can recover the underlying true data density. However, it still needs to assume the model has infinite modeling capacity to prove the result in a non-parametric fashion. This is probably due to the use of a fixed margin to separate generated samples from training examples. This is in contrast to the use of a distance metric in the proposed LS-GAN to specify data-dependent margins under the Lipschitz density assumption. In addition, [8] presented to analyze the GAN from information-theoretic perspective, and they seek to minimize the variational estimate of f -divergence, and show that the classic GAN is included as a special case of f -GAN. In contrast, InfoGAN [9] proposed another information-theoretic GAN to learn disentangled representations capturing various latent concepts and factors in generating samples.

Besides the class of GANs, there exist other models that also attempt to generate natural images. For example, [10] rendered images by matching features in a convolutional network with respect to reference images. [11] used deconvolutional network to render 3D chair models in various styles and viewpoints. [12] introduced a deep recurrent neural network architecture for image generation with a sequence of variational auto-encoders to iteratively construct complex images.

Recent efforts have been made to leverage the learned representations by deep generative networks to improve the classification accuracy when it is too difficult or expensive to label sufficient training examples. For example, [13] presented variational auto-encoders [14] by combining deep generative models and approximate variational inference to explore both labeled and unlabeled data. [3] treated the samples from the GAN generator as a new class, and explore unlabeled examples by assigning them to a class different from the new one. [15] proposed to train a ladder network [16] by minimizing the sum of supervised and unsupervised cost functions through back-propagation, which avoids the conventional layer-wise pre-training approach. [17] presented an approach to learning a discriminative classifier by trading-off mutual information between observed examples and their predicted classes against an adversarial generative model. These methods have shown promising results for classification tasks by leveraging deep generative networks or their generated samples.

In this paper, we seek to develop models and algorithms that are both theoretically sound and practically competitive for data generation and classification tasks. Our contributions are summarized below.

- We propose a Loss-Sensitive GAN (LS-GAN) model to produce high-quality samples. The LS-GAN learns a loss function to quantify the quality of generated

samples. The loss of a real example should be smaller than that of a generated sample by a margin characterized by their distance in a metric space. The well generated samples close to real examples do not need to be treated as negative examples anymore so that more efforts can be focused on improving the quality of poor samples.

- We also generalize LS-GAN to a conditional version that shares the same theoretical merit as the LS-GAN but can generate samples aligned with designed conditions. Specifically, we consider to specify sample classes as conditions, and this model can produce multiple classes of examples that capture intra-class variations. This yields a classifier using the learned loss function and exploring the generated samples to improve classification accuracy.
- We develop a new theory that introduces Lipschitz assumption to characterize underlying data densities. We will prove the LS-GAN can reveal the true density even with limited modeling ability of bounded Lipschitz constant on the generators and loss functions. This is a nontrivial relaxation of the assumption on the classic GAN that assumes infinite modeling ability in the theoretical analysis. Moreover, we also characterize the learned loss function by deriving its lower and upper bounds, which may shed some light on a principled criterion to regularize the model.

3 LOSS-SENSITIVE GAN

In the proposed LS-GAN, we abandon to learn a discriminator that uses a probability to characterize the likelihood of real samples. Instead, we introduce a loss function $L_\theta(\mathbf{x})$ to distinguish real and generated samples by the assumption that a real sample should have a smaller value of the loss function than a generated counterpart.

We require the loss function should be lower bounded by zero. Without loss of generality, any lower bounded function can be translated to have a lower bound of zero. Along with such a loss function, a generator $G_\phi(\mathbf{z})$ will also be learned by minimizing the loss to produce real data samples with random prior \mathbf{z} from a distribution $P_z(\mathbf{z})$.

Formally, consider a real example \mathbf{x} and a generated one $G_\phi(\mathbf{z})$ with $\mathbf{z} \sim P_z(\mathbf{z})$. The loss function can be trained by the following constraint:

$$L_\theta(\mathbf{x}) \leq L_\theta(G_\phi(\mathbf{z})) - \Delta(\mathbf{x}, G_\phi(\mathbf{z})) \quad (1)$$

where $\Delta(\mathbf{x}, G_\phi(\mathbf{z}))$ measures the difference between \mathbf{x} and $G_\phi(\mathbf{z})$. This constraint requires a real sample be separated from a generated counterpart in terms of their losses by at least a margin of $\Delta(\mathbf{x}, G_\phi(\mathbf{z}))$. Figure 1 illustrates this idea.

It is noteworthy that the margin is not fixed to a constant. Instead, it is data-dependent, which could vanish as the generator is gradually improved to produce better samples as they become closer to real examples. For example, one can choose the ℓ_p -distance $\|\mathbf{x} - G_\phi(\mathbf{z})\|_p$ as the margin. This allows the model to focus on improving the poor samples still far away from real examples rather than wasting efforts on those that are already well generated. In the theoretical analysis, such a data-dependent margin will also be used to

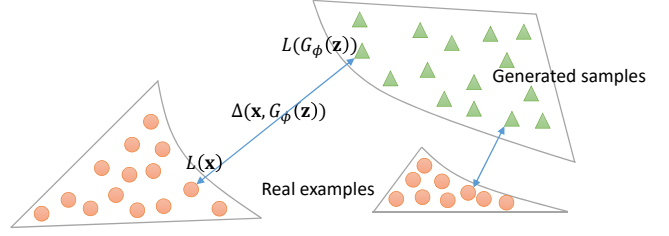


Fig. 1. Illustration of the idea behind LS-GAN. A margin is enforced to separate real samples from generated counterparts. The margin is not fixed to a constant. Instead it is data-dependent, which could vanish as the generator improves to produce better and better samples. We assume the density of real samples is Lipschitz as to prove the theoretical results.

specify a Lipschitz condition, which plays a critical role in guaranteeing generated samples follow the underlying data density.

Now let us relax the above hard constraint by introducing a slack variable $\xi_{\mathbf{x}, \mathbf{z}}$

$$L_\theta(\mathbf{x}) - \xi_{\mathbf{x}, \mathbf{z}} \leq L_\theta(G_\phi(\mathbf{z})) - \Delta(\mathbf{x}, G_\phi(\mathbf{z})) \quad (2)$$

$$\xi_{\mathbf{x}, \mathbf{z}} \geq 0 \quad (3)$$

where the slack variable would be nonzero when a violation of the constraint occurs.

Therefore, with a fixed generator G_ϕ , the loss function parameterized with θ can be trained by

$$\begin{aligned} \min_{\theta} \quad & \mathbb{E}_{\mathbf{x} \sim P_{data}(\mathbf{x})} L_\theta(\mathbf{x}) + \lambda \mathbb{E}_{\substack{\mathbf{x} \sim P_{data}(\mathbf{x}) \\ \mathbf{z} \sim P_z(\mathbf{z})}} \xi_{\mathbf{x}, \mathbf{z}} \\ \text{s.t.,} \quad & L_\theta(\mathbf{x}) - \xi_{\mathbf{x}, \mathbf{z}} \leq L_\theta(G_\phi(\mathbf{z})) - \Delta(\mathbf{x}, G_\phi(\mathbf{z})) \\ & \xi_{\mathbf{x}, \mathbf{z}} \geq 0 \end{aligned} \quad (4)$$

where λ is a positive balancing parameter, and $P_{data}(\mathbf{x})$ is the data distribution for real samples. The first term of the objective function minimizes the expected loss function over data distribution as a smaller value of loss function is preferred on real samples. The second term is the expected error caused by the violation of the constraint.

On the other hand, for a fixed loss function L_θ , one can solve the following minimization problem to find an optimal generator.

$$\min_{\phi} \mathbb{E}_{\substack{\mathbf{x} \sim P_{data}(\mathbf{x}) \\ \mathbf{z} \sim P_z(\mathbf{z})}} L_\theta(G_\phi(\mathbf{z})) \quad (5)$$

This problem directly minimizes $L_\theta(G_\phi(\mathbf{z}))$. However, when $L_\theta(G_\phi(\mathbf{z}))$ is large, it now can provide sufficient gradient to update ϕ .

In summary, L_θ and G_ϕ are alternately optimized by solving a Nash equilibrium (θ^*, ϕ^*) such that θ^* minimizes

$$\begin{aligned} S(\theta, \phi^*) = & \mathbb{E}_{\mathbf{x} \sim P_{data}(\mathbf{x})} L_\theta(\mathbf{x}) \\ & + \lambda \mathbb{E}_{\substack{\mathbf{x} \sim P_{data}(\mathbf{x}) \\ \mathbf{z}_G \sim P_{G^*}(\mathbf{z}_G)}} (\Delta(\mathbf{x}, \mathbf{z}_G) + L_\theta(\mathbf{x}) - L_\theta(\mathbf{z}_G))_+ \end{aligned} \quad (6)$$

and ϕ^* minimizes

$$T(\theta^*, \phi) = \mathbb{E}_{\mathbf{z}_G \sim P_G(\mathbf{z}_G)} L_{\theta^*}(\mathbf{z}_G) \quad (7)$$

where $P_G(\mathbf{z}_G)$ is the density of samples generated by $G_\phi(\mathbf{z})$.

4 THEORETICAL ANALYSIS

Suppose (θ^*, ϕ^*) is a Nash equilibrium that jointly solves (6) and (7). We will show that as $\lambda \rightarrow +\infty$, the density distribution P_{G^*} of the samples generated by G_{ϕ^*} will converge to the underlying data density P_{data} .

To prove this result, we have the following definition

Definition. For any two samples \mathbf{x} and \mathbf{z} , the loss function $F(\mathbf{x})$ is Lipschitz continuous with respect to a distance metric Δ if

$$|F(\mathbf{x}) - F(\mathbf{z})| \leq \kappa \Delta(\mathbf{x}, \mathbf{z})$$

with a bounded Lipschitz constant κ , i.e., $\kappa < +\infty$.

To prove our main result, we have the following assumption

Assumption 1. The data density P_{data} is supported in a compact set, and it is Lipschitz continuous.

The set of Lipschitz densities in a compact support contain a large family of distributions that are dense in the space of continuous densities. For example, the density of natural images can be considered as Lipschitz continuous, as the densities of two similar images in a neighborhood are unlikely to change abruptly. Moreover, one can restrict the image density in a compact support as an image has bounded pixel values on $[0, 255]$.

This is contrary to the analysis of the classic GAN, where one must assume both discriminator and generator have infinite modeling ability to prove P_{G^*} equals P_{data} . The Lipschitz assumption on the data density allows us to relax such a strong assumption to Lipschitz loss function L_θ and generator density P_G . This results in the following lemma relating P_{G^*} to P_{data} .

Lemma 1. Under Assumption 1, given a Nash equilibrium (θ^*, ϕ^*) such that P_{G^*} is Lipschitz continuous, we have

$$\int_{\mathbf{x}} |P_{data}(\mathbf{x}) - P_{G^*}(\mathbf{x})| d\mathbf{x} \leq \frac{2}{\lambda}$$

Thus, $P_{G^*}(\mathbf{x})$ converges to $P_{data}(\mathbf{x})$ as $\lambda \rightarrow +\infty$.

The proof of this lemma is given in the appendix.

Now we can show the existence of Nash equilibrium such that both the loss function L_θ and the density $P_G(\mathbf{z}_G)$ of generated samples are Lipschitz.

Let \mathcal{F}_κ be the class of functions with a bounded Lipschitz constant κ . It is not difficult to show that the space \mathcal{F}_κ is convex and compact if these functions are supported in a compact set¹. In addition, both $S(\theta, \phi)$ and $T(\theta, \phi)$ are convex functions in L_θ and in $P_G(\mathbf{z}_G)$. These guarantee the existence of a Nash equilibrium (θ^*, ϕ^*) with both L_{θ^*} and P_{G^*} in \mathcal{F}_κ , following the proof of the classic mixed-strategy game theory by applying Kakutani fixed-point theorem [18]. Thus, we have the following lemma.

Lemma 2. Under Assumption 1, there exists a Nash equilibrium (θ^*, ϕ^*) such that L_{θ^*} and P_{G^*} are Lipschitz.

Putting the above two lemmas together, we have the following theorem.

Theorem 1. Under Assumption 1, a Nash equilibrium (θ^*, ϕ^*) exists such that

1. For example, the space of natural images is compact as their pixel values are restricted to a compact range of $[0, 255]$.

(i) L_{θ^*} and P_{G^*} are Lipschitz.

(ii) $\int_{\mathbf{x}} |P_{data}(\mathbf{x}) - P_{G^*}(\mathbf{x})| d\mathbf{x} \leq \frac{2}{\lambda} \rightarrow 0$, as $\lambda \rightarrow +\infty$;

(iii) $P_{data}(\mathbf{x}) \geq \frac{\lambda}{1 + \lambda} P_{G^*}(\mathbf{x})$.

5 ALGORITHM

The above minimization problems (6) and (7) can be rewritten by replacing the expectation with a given set of examples $\mathcal{X}_n = \{\mathbf{x}_1, \dots, \mathbf{x}_n\}$ and the noise vectors $\mathcal{Z}_m = \{\mathbf{z}_1, \dots, \mathbf{z}_m\}$ drawn from a distribution $P_z(\mathbf{z})$.

This results in the following two problems.

$$\begin{aligned} \min_{\theta} S_{n,m}(\phi^*, \theta) &\triangleq \frac{1}{n} \sum_{i=1}^n L_\theta(\mathbf{x}_i) \\ &+ \frac{\lambda}{nm} \sum_{i,j=1}^{n,m} (\Delta(\mathbf{x}_i, G_{\phi^*}(\mathbf{z}_j)) + L_\theta(\mathbf{x}_i) - L_\theta(G_{\phi^*}(\mathbf{z}_j)))_+ \end{aligned} \quad (8)$$

and

$$\min_{\phi} T_n(\theta^*, \phi) = \frac{1}{k} \sum_{i=1}^k L_{\theta^*}(G_\phi(\mathbf{z}'_i)) \quad (9)$$

The random vectors $\mathcal{Z}'_k = \{\mathbf{z}'_i | i = 1, \dots, k\}$ used in (9) can be different from \mathcal{Z}_m used in (8).

The choice of a generator G_ϕ is task dependent. For example, if one wishes to generate images, a convolutional neural network can be used to synthesize images from low to high resolution. Many research efforts have been made to design various generator architectures. We refer the readers to [2], [5] for more choices of generator architectures.

On the other hand, we can also choose a deep network to compute the loss function $L_\theta(\mathbf{x})$. For example, one can choose $L_\theta(\mathbf{x}) = -\log \sigma(a(\mathbf{x}))$ with a sigmoid activation $a(\mathbf{x})$ produced by a multi-layer neural network, with $\sigma(a(\mathbf{x}))$ being explained as the probability of the input \mathbf{x} being real. However, sticking to a probabilistic explanation is unnecessary, and any loss function lower bounded by zero can be used. For example, a rectifier activation function can be added to the top of a neural network to output the loss.

The loss function and the generator can be learned by alternating between the two problems over mini-batches. In each mini-batch, a set \mathcal{Z}_m of random noises are sampled from a prior distribution $P_z(\mathbf{z})$, along with a subset of real samples from the training set \mathcal{X}^n . Then, the loss function is updated by descending the gradient of (8), and the generator is updated by minimizing (9) with a set of random vectors \mathcal{Z}'_k sampled from $P_z(\mathbf{z})$. After the generator G_{ϕ^*} has been updated, the data points $\mathbf{x}^{(n+j)} = G_{\phi^*}(\mathbf{z}_j)$ of generated samples will also be updated. Algorithm 1 summarizes the learning algorithm for the LS-GAN.

5.1 Characterization of Loss functions

Now let us characterize the optimal loss functions based on the objective (8), which will provide us an insight into the LS-GAN algorithm. For this purpose, we consider non-parametric solutions by generalizing the non-parametric maximum likelihood in [19] to minimize (8) over the whole class of Lipschitz loss functions. We will show that these solutions provide an upper and a lower bound of loss functions to be sought by (8).

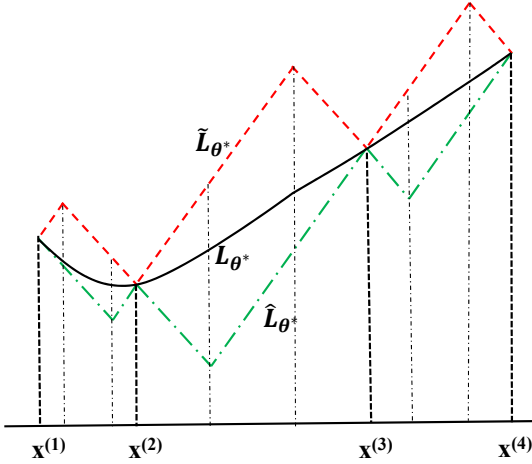


Fig. 2. Comparison between two optimal loss functions \tilde{L}_{θ^*} and \hat{L}_{θ^*} for LS-GAN. They are upper and lower bounds of the class of optimal loss functions L_{θ^*} to Problem (8). The values of all optimal loss functions coincide on the data points $\mathbf{x}^{(i)}$, $i = 1, \dots, n+m$.

Let $\mathbf{x}^{(1)} = \mathbf{x}_1, \mathbf{x}^{(2)} = \mathbf{x}_2, \dots, \mathbf{x}^{(n)} = \mathbf{x}_n, \mathbf{x}^{(n+1)} = G_{\phi^*}(\mathbf{z}_1), \dots, \mathbf{x}^{(n+m)} = G_{\phi^*}(\mathbf{z}_m)$, i.e., the first n data points are real examples and the rest m are generated samples. Then we have the following theorem.

Theorem 2. *The following functions \hat{L}_{θ^*} and \tilde{L}_{θ^*} both minimize $S_{n,m}(\theta, \phi^*)$ in \mathcal{F}_κ :*

$$\begin{aligned} \hat{L}_{\theta^*}(\mathbf{x}) &= \max_{1 \leq i \leq n+m} \{ (l_i^* - \kappa \Delta(\mathbf{x}, \mathbf{x}^{(i)}))_+ \}, \\ \tilde{L}_{\theta^*}(\mathbf{x}) &= \min_{1 \leq i \leq n+m} \{ l_i^* + \kappa \Delta(\mathbf{x}, \mathbf{x}^{(i)}) \} \end{aligned} \quad (10)$$

with the same group of parameters $\theta^* = [l_1^*, \dots, l_{n+m}^*] \in \mathbb{R}^{n+m}$. They are supported in the convex hull of $\{\mathbf{x}^{(1)}, \dots, \mathbf{x}^{(n+m)}\}$, and we have

$$\hat{L}_{\theta^*}(\mathbf{x}^{(i)}) = \tilde{L}_{\theta^*}(\mathbf{x}^{(i)}) = l_i^*$$

for $i = 1, \dots, n+m$, i.e., their values coincide on $\{\mathbf{x}^{(1)}, \mathbf{x}^{(2)}, \dots, \mathbf{x}^{(n+m)}\}$.

The proof of this theorem is given in the appendix.

From the theorem, it is not hard to show that any convex combination of these two forms attains the same value of $S_{n,m}$, and is also its global minimizer. Thus, we have the following corollary.

Corollary 1. *All the functions in*

$$\mathcal{L}_{\theta^*} = \{\gamma \hat{L}_{\theta^*} + (1 - \gamma) \tilde{L}_{\theta^*} \mid 0 \leq \gamma \leq 1\} \subset \mathcal{F}_\kappa$$

are the global minimizer of $S_{n,m}$ in \mathcal{F}_κ .

This shows that the global minimizer is not unique. Moreover, through the proof of Theorem 2, one can find that $\tilde{L}_{\theta^*}(\mathbf{x})$ and $\hat{L}_{\theta^*}(\mathbf{x})$ are the upper and lower bound of any optimal loss function solution to the problem (8). In particular, we have the following corollary.

Corollary 2. *For any $L_{\theta^*}(\mathbf{x}) \in \mathcal{F}_\kappa$ that minimizes $S_{n,m}$, the corresponding $\hat{L}_{\theta^*}(\mathbf{x})$ and $\tilde{L}_{\theta^*}(\mathbf{x})$ are the lower and upper bounds of $L_{\theta^*}(\mathbf{x})$, i.e.,*

$$\hat{L}_{\theta^*}(\mathbf{x}) \leq L_{\theta^*}(\mathbf{x}) \leq \tilde{L}_{\theta^*}(\mathbf{x})$$

The proof is given in Appendix B.

The parameters $\theta^* = [l_1^*, \dots, l_{n+m}^*]$ in (10) can be sought by minimizing

$$\begin{aligned} S_{n,m}(\phi^*, \theta) &\triangleq \frac{1}{n} \sum_{i=1}^n l_i + \frac{\lambda}{nm} \sum_{i,j=1}^{n,m} (\Delta_{i,n+j} + l_i - l_{n+j})_+ \\ \text{s.t., } |l_i - l_{i'}| &\leq \kappa \Delta(\mathbf{x}^{(i)}, \mathbf{x}^{(i')}) \\ l_i &\geq 0, i, i' = 1, \dots, n+m \end{aligned} \quad (11)$$

where $\Delta_{i,j}$ is short for $\Delta(\mathbf{x}^{(i)}, \mathbf{x}^{(n+j)})$, and the constraints are imposed to ensure the learned loss functions stay in \mathcal{F}_κ . With a greater value of κ , a larger class of loss function will be sought. Thus, one can control the modeling ability of the loss function by setting a proper value to κ .

Problem (11) is a typical linear programming problem. In principle, one can solve this problem to obtain a non-parametric loss function for the LS-GAN. Unfortunately, it consists of a large number of constraints, whose scale is at an order of $\binom{n+m}{2}$. This prevents us from using (11) directly to solve an optimal LS-GAN model with a very large number of training examples.

However, this non-parametric solution has theoretical value in characterizing the loss function learned by a deep network. As illustrated in Figure 2, the values of any optimal loss functions should coincide on the sampled data points $\mathbf{x}^{(i)}$, $i = 1, \dots, n+m$, and the values between these points are bounded between $\tilde{L}_{\theta^*}(\mathbf{x})$ and $\hat{L}_{\theta^*}(\mathbf{x})$. With a greater value of Lipschitz constant κ , a large space of loss functions are sought between these two bounds.

This sheds light on a principled approach to regularize the complexity of the LS-GAN by controlling its Lipschitz constant. It is known by the mean-value theorem that the Lipschitz constant κ of a function is bounded by the norm of its gradient on the domain. Hence, one can monitor the gradient norm to predict if it is out of normal range and the model starts to become overcomplex with a too large functional space. If so, a mechanism can be adopted to control κ . For example, weight decay usually can reduce the gradient norm indirectly as the network weights are reduced. Alternatively, one may consider to directly minimize the gradient norm $\|\nabla_{\mathbf{x}} \hat{L}_{\theta}(\mathbf{x})\|$ as a regularizer for the LS-GAN. In this paper, we adopt weight decay for its simplicity and find it works well with the LS-GAN model in experiments.

6 CONDITIONAL LS-GAN

The LS-GAN can easily be generalized to produce a sample based on a given condition \mathbf{y} , yielding a new paradigm of Conditional LS-GAN (CLS-GAN).

For example, if the condition is an image class, the CLS-GAN seeks to produce images of the given class; otherwise, if a text description is given as a condition, the model attempts to generate images aligned with the given description. This gives us more flexibility in controlling what samples to be generated.

Formally, the generator of CLS-GAN takes a condition vector \mathbf{y} as input along with a noise vector \mathbf{z} to produce a sample $G_\phi(\mathbf{z}, \mathbf{y})$. To train the model, we define a loss

Algorithm 1 Learning algorithm for LS-GAN.

```

Input:  $n$  data examples  $\mathcal{X}_n$ , and  $\lambda$ .
for a number of iterations do
  for a number of steps do
    \\Update the loss function over minibatches;
    Sample a minibatch from  $\mathcal{X}_n$ ;
    Sample a minibatch from  $\mathcal{Z}_m$ ;
    Update the loss function  $L_\theta$  by descending the gradient
    of (8) with weight decay over the minibatches;
  end for
  Sample a set of  $\mathcal{Z}'_k$  of  $k$  random noises;
  Update the generator  $G_\phi$  by descending the gradient of
  (9) with weight decay;
  Update the generated samples  $\mathbf{x}^{(n+j)} = G_{\phi^*}(\mathbf{z}_j)$  for
   $j = 1, \dots, m$  on  $\mathcal{Z}_m$ ;
end for

```

function $L_\theta(\mathbf{x}, \mathbf{y})$ to measure the degree of the misalignment between a data sample \mathbf{x} and a given condition \mathbf{y} .

For a real example \mathbf{x} aligned with the condition \mathbf{y} , its loss function should be smaller than that of a generated sample by a margin of $\Delta(\mathbf{x}, G_\phi(\mathbf{z}, \mathbf{y}))$. This results in the following constraint,

$$L_\theta(\mathbf{x}, \mathbf{y}) \leq L_\theta(G_\phi(\mathbf{z}, \mathbf{y}), \mathbf{y}) - \Delta(\mathbf{x}, G_\phi(\mathbf{z}, \mathbf{y})) \quad (12)$$

Like the LS-GAN, this type of constraint yields the following non-zero-sum game to train the CLS-GAN, which seeks a Nash equilibrium (θ^*, ϕ^*) so that θ^* minimizes

$$S(\theta, \phi^*) = \mathbb{E}_{\mathbf{x}, \mathbf{y} \sim P_{data}(\mathbf{x}, \mathbf{y})} L_\theta(\mathbf{x}, \mathbf{y}) + \lambda \mathbb{E}_{\substack{\mathbf{x}, \mathbf{y} \sim P_{data}(\mathbf{x}, \mathbf{y}) \\ \mathbf{z} \sim P_z(\mathbf{z})}} (\Delta(\mathbf{x}, G_{\phi^*}(\mathbf{z}, \mathbf{y})) + L_\theta(\mathbf{x}, \mathbf{y}) - L_\theta(G_{\phi^*}(\mathbf{z}, \mathbf{y}), \mathbf{y}))_+$$
(13)

and ϕ^* minimizes

$$T(\theta^*, \phi) = \mathbb{E}_{\substack{\mathbf{y} \sim P_{data}(\mathbf{y}) \\ \mathbf{z} \sim P_z(\mathbf{z})}} L_{\theta^*}(G_\phi(\mathbf{z}, \mathbf{y}), \mathbf{y}) \quad (14)$$

Playing the above game will lead to a trained pair of loss function L_{θ^*} and generator G_{ϕ^*} . We can show that the learned generator $G_{\phi^*}(\mathbf{z}, \mathbf{y})$ can produce samples whose distribution follows the true data density $P_{data}(\mathbf{x}|\mathbf{y})$ for a given condition \mathbf{y} .

To prove this, we say a loss function $L_\theta(\mathbf{x}, \mathbf{y})$ is Lipschitz if it is Lipschitz continuous in its first argument \mathbf{x} . We make the following assumption.

Assumption 2. For each \mathbf{y} , the conditional density $P_{\text{data}}(\mathbf{x}|\mathbf{y})$ is Lipschitz, and is supported in a convex compact set of \mathbf{x} .

Then it is not difficult to prove the following theorem, which shows that the conditional density $P_{G^*}(\mathbf{x}|\mathbf{y})$ becomes $P_{data}(\mathbf{x}|\mathbf{y})$ as $\lambda \rightarrow +\infty$. Here $P_{G^*}(\mathbf{x}|\mathbf{y})$ denotes the density of samples generated by $G_{\phi^*}(\mathbf{z}, \mathbf{y})$ with sampled random noise \mathbf{z} .

Theorem 3. Under Assumption 2, a Nash equilibrium (θ^*, ϕ^*) exists such that

(i) $L_{\theta^*}(\mathbf{x}, \mathbf{y})$ is Lipschitz continuous in \mathbf{x} for each \mathbf{y} ;

(ii) $P_{G^*}(\mathbf{x}|\mathbf{y})$ is Lipschitz continuous;
 (iii) $\int_{\mathbf{x}} |P_{data}(\mathbf{x}|\mathbf{y}) - P_{G^*}(\mathbf{x}|\mathbf{y})| d\mathbf{x} \leq \frac{2}{\lambda}.$

In addition, similar upper and lower bounds can be derived to characterize the learned conditional loss function $L_\theta(\mathbf{x}, \mathbf{y})$ following the same idea for LS-GAN.

A useful byproduct of the CLS-GAN is one can use the learned loss function $L_{\theta^*}(\mathbf{x}, \mathbf{y})$ to predict the label of an example \mathbf{x} by

$$\mathbf{y}^* = \arg \min_{\mathbf{y}} L_{\theta^*}(\mathbf{x}, \mathbf{y}) \quad (15)$$

The advantage of such a CLS-GAN classifier is it is trained with both labeled and generated examples, the latter of which can regulate the training of the classifier by covering more potential variations for different classes. It also provides a way to evaluate the model based on its classification performance. This is an objective metric we can use to assess the quality of feature representations learned by the model.

For a classification task, a suitable value should be set to λ . Although Theorem 3 shows P_{G^*} would converge to the true conditional density P_{data} by increasing λ , a too large value of λ tends to ignore the first loss minimization term of (13) that plays an important role in minimizing classification error. In the experiments, we will make a balance between classification and generation by tuning a proper value to λ on an independent validation set or via a cross-validation process.

7 EXPERIMENTS

Objective evaluation of a data generative model is not an easy task as there is no consensus criteria to quantify the quality of generated samples. For this reason, we use image classification as a surrogate to quantitatively evaluate the resultant LS-GAN model, along with qualitative evaluation of the generated images.

First, we will perform an objective evaluation by using the learned loss function in the CLS-GAN to classify images. This task evaluates the quality of the feature representations extracted by the CLS-GAN in terms of its classification accuracy directly. We will compare it with the feature representations extracted by the other deep generative networks.

Moreover, we will conduct a qualitative evaluation of the generated images, and analyze the factors that would affect image generation performance. It will give us an intuitive idea of why and how the LS-GAN can capture class-invariant feature representations to classify and generate images for various classes.

7.1 Architectures

The detail of the network architecture we adopt for training CLS-GAN on these two datasets is presented in Table 1.

Specifically, we adopt the ideas behind the network architecture for the DCGAN [2] to build the generator and the loss function networks. Compared with the conventional CNNs, maxpooling layers are replaced with strided convolutions in both networks, and fractionally-strided convolutions are used in the generator network to upsample feature maps across layers to finer resolutions. Batch-normalization layers are added in both networks between convolutional

TABLE 1

The Network architecture used in LS-GAN for training CIFAR-10 and SVHN, where BN stands for batch normalization, LeakyReLU for Leaky Rectifier with a slope of 0.2 for negative value, and “3c1s96o Conv.” means a 3×3 convolution kernel with stride 1 and 96 outputs, while “UpConv.” denotes the fractionally-stride convolution.

(a) Loss Function Network
Input $32 \times 32 \times 3$
3c1s96o Conv. BN LeakyReLU
3c1s96o Conv. BN LeakyReLU
4c2s96o Conv. BN LeakyReLU
3c1s192o Conv. BN LeakyReLU
3c1s192o Conv. BN LeakyReLU
4c2s192o Conv. BN LeakyReLU
3c1s192o Conv. BN LeakyReLU
3c1s192o Conv. BN LeakyReLU
1c1s192o Conv. BN LeakyReLU
global meanpool
Output $32 \times 32 \times 10$

(b) Generator Network
Input 100-D random vector + 10-D one-hot vector
4c1s512o UpConv. BN LeakyReLU
4c2s256o UpConv. BN LeakyReLU
4c2s128o UpConv. BN LeakyReLU
4c2s3o UpConv. BN LeakyReLU
Elementwise Tanh
Output $32 \times 32 \times 3$

layers, and fully connected layers are removed from these networks.

For the loss function network in CLS-GAN, a global mean-pooling layer is added on top of convolutional layers. This produces a 1×1 feature map that is fed into a cross-entropy cost function to produce the loss $L_\theta(\mathbf{x}, \mathbf{y})$ conditioned on a given class \mathbf{y} .

In the generator network, Tanh is used to produce images whose pixel values are scaled to $[-1, 1]$. Thus, all image examples in datasets are preprocessed to have their pixel values in $[-1, 1]$. More details about the design of network architectures can be found in literature [2]. Table 1 shows the network architecture for the LS-GAN model on CIFAR-10 and SVHN datasets in the experiments. In particular, the architecture of the loss function network is adapted from that used in [17] with nine hidden layers.

7.2 Training Details

The models are trained in a mini-batch of 64 images, and their weights are initialized from a zero-mean Gaussian distribution with a standard deviation of 0.02. The Adam optimizer [20] is used to train the network with initial learning rate and β_1 being set to 10^{-3} and 0.5 respectively, while the learning rate is annealed every 25 epochs by a factor of 0.8.

The hyperparameter γ and the weight decay rate is chosen via a five-fold cross-validation. We also test different types of distance functions for $\Delta(\cdot, \cdot)$ in the model, and find pixel-wise L_1 distance achieves better performance

than the other compared choices like L_2 distance. Thus we choose L_1 distance through the experiments. We also tried intermediate feature maps from the loss function network to compute the distance between images as the margin. But we find the results are not as good as the L_1 distance. We found that these intermediate feature maps would collapse to the same map across images as the margin $\Delta(\cdot, \cdot)$ reduces to zero through training.

For the generator network of CLS-GAN, it tasks a 100-dimensional random vector drawn from $\text{Unif}[-1, 1]$ as input that is concatenated with an one-hot vector encoding the image class. We will train CLS-GAN as presented in Section 6 by involving labeled training examples. This will be compared against the other state-of-the-art supervised deep generative models as well as the other GAN models in literature.

7.3 Image Classification

We conduct experiments on CIFAR-10 and SVHN to compare the classification accuracy of LS-GAN with the other approaches.

7.3.1 CIFAR-10

The CIFAR dataset [25] consists of 50,000 training images and 10,000 test images on ten image categories. We test the proposed CLS-GAN model with supervised labels as conditions. In the supervised training, all labeled examples are used to train the CLS-GAN. We also conduct experiments with 400 labeled examples per class, which is a more challenging task as much fewer labeled examples are used for training. The experiment results on this task are reported by averaging over ten random subsets of labeled examples.

We compare the proposed model with the state-of-the-art methods in literature. In particular, we compare with the conditional GAN [24] as well as the DCGAN [2]. For the sake of fair comparison, the conditional GAN shares the same architecture as the CLS-GAN except the CLS-GAN is trained with the loss-sensitive objective, while the conditional GAN is trained in a supervised fashion by minimizing cross-entropy cost together with the GAN cost. Both conditional GAN and CLS-GAN are trained in a fully supervised fashion, making it possible to perform a direct comparison between their classification accuracies. On the other hand, the DCGAN algorithm [2] max-pools the discriminator’s convolution features from all layers to 4×4 grids as the image features, and a L2-SVM is then trained to classify images. The DCGAN is an unsupervised model which has shown competitive performance on generating photo-realistic images. Its feature representations are believed to reach the state-of-the-art performance in modeling images with no supervision.

We also compare with the other recently developed models in literature, including the baseline 1 Layer K-means feature extraction pipeline, a multi-layer extension of the baseline model (3 Layer K-means Learned RF [21]), View Invariant K-means [22], Examplar CNN [23], Ladder Network [15] and CatGAN [17]. Table 2 compares the experiment results, showing the CLS-GAN successfully outperforms these compared algorithms.

TABLE 2

Classification results on CIFAR-10 dataset, in comparison with state-of-the-art methods. The best result is highlight in bold.

Methods		Accuracy (All)	Accuracy (400 per class)
1 Layer K-means [2]		80.6%	63.7% ($\pm 0.7\%$)
3 Layer K-means Learned RF [21]		82.0%	70.7% ($\pm 0.7\%$)
View Invariant K-means [22]		81.9%	72.6% ($\pm 0.7\%$)
Exemplar CNN [23]		84.3%	77.4% ($\pm 0.2\%$)
Conditional GAN [24]		83.6%	75.5% ($\pm 0.4\%$)
DCGAN [2]		82.8%	73.8% ($\pm 0.4\%$)
Ladder Network [15]		—	79.6% ($\pm 0.5\%$)
CatGAN [17]		—	80.4% ($\pm 0.4\%$)
CLS-GAN		91.7%	81.8% ($\pm 0.4\%$)

TABLE 3

Classification results on SVHN dataset with 1,000 labeled examples. The best result is highlighted in bold.

Methods		Error rate
KNN [2]		77.93%
TSVM [2]		66.55%
M1+KNN [13]		65.63%
M1+TSVM [13]		54.33%
M1+M2 [13]		36.02%
SWWAE w/o dropout [27]		27.83%
SWWAE with dropout [27]		23.56%
DCGAN [2]		22.48%
Conditional GAN [24]		21.85% $\pm 0.38\%$
Supervised CNN [2]		28.87%
DGN [13]		36.02% $\pm 0.10\%$
Virtual Adversarial [28]		24.63%
Auxiliary DGN [29]		22.86%
Skip DGN [29]		16.61% $\pm 0.24\%$
CLS-GAN		13.74% $\pm 0.32\%$

7.3.2 SVHN

The SVHN (i.e., Street View House Number) dataset [26] contains 32×32 color images of house numbers collected by Google Street View. They are roughly centered on a digit in a house number, and the objective is to recognize the digit. The training set has 73,257 digits while the test set consists of 26,032.

To test the model, 1,000 labeled digits are used to train the model, which are uniformly selected from ten digit classes, that is 100 labeled examples per digit class. This is a very challenging classification task as very rare examples are used to train the model. We expect a good generative model could produce additional examples to augment the training set.

We use the same experiment setup and network architecture for CIFAR-10 dataset. Table 3 reports the results on the SVHN dataset. It shows that LS-GAN outperforms the compared algorithms again.

7.4 Analysis of Generated Images

Figure 3 illustrates the generated images by CLS-GAN for MNIST, CIFAR-10 and SVHN datasets. On each dataset, images in a column are generated for the same class. On the MNIST and the SVHN, both handwritten and street-view digits are quite legible. Both also cover many variants

for each digit class. For example, the synthesized MNIST digits have various writing styles, rotations and sizes, and the generated SVHN digits have various lighting conditions, sizes and even different co-occurring digits. For the generated CIFAR-10 images, most of their classes are recognizable even though some visual details are missing. This is because the training examples on CIFAR-10 only have very limited resolution (32×32 pixels), and there should be a large room to render more details if higher-resolution examples were available.

We also observe that if we set a small value to the hyperparameter λ , the generated images would become very similar to each other within each class. As illustrated in Figure 4, the images are generated by halving λ used for generating images in Figure 3. A smaller λ means a relatively large weight is placed on the first loss minimization term of (8), which tends to collapse generated images to a single mode as it aggressively minimizes their losses to train the generator. This is also consistent with Theorem 3 where the density of generated samples with a smaller λ could have a larger deviation from the underlying density. One should avoid the collapse of trained generator since diversifying generated images can improve the classification performance of the CLS-GAN by revealing more intra-class variations. This will help improve the model’s generalization ability as these variations could appear in future images.

However, one should also avoid setting too large value to λ . Otherwise, the role of the first loss minimization term could be underestimated, which can also adversely affect the classification results without reducing the training loss to a satisfactory level. Therefore, we choose a proper value for λ by cross-validation on the training set from {1.0, 2.5, 5.0, 10.0} in the experiments.

In brief, the comparison between Figure 3 and Figure 4 reveals a trade-off between image generation quality and classification accuracy through the hyperparameter λ . Such a trade-off is intuitive: while a classification task usually focuses on learning class-invariant representations that do not change within a class, image generation should be able to capture class-variant factors (e.g., lighting conditions, viewing angles, and object poses) so that it could diversify generated samples for each class. Although diversified examples can augment training dataset, it comes at a cost of trading class-invariance for modeling variant generation factors. Perhaps, this is an intrinsic dilemma between su-

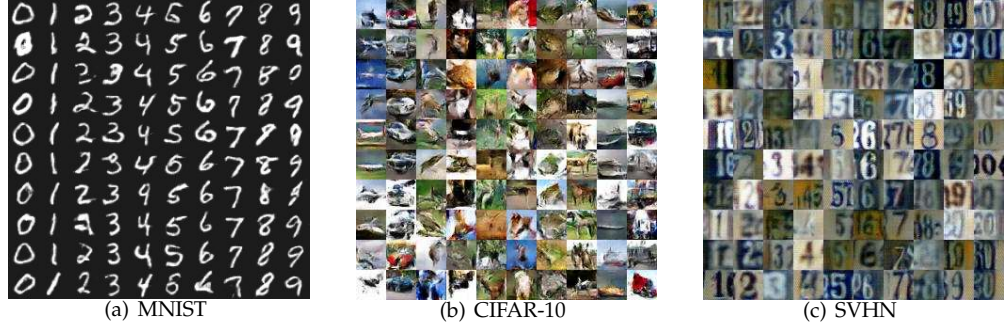


Fig. 3. Images generated by CLS-GAN for MNIST, CIFAR-10 and SVHN datasets. For each dataset, images in a column are generated according to the same class. In particular, the generated CIFAR-10 images are airplane, automobile, bird, cat, deer, dog, frog, horse, ship and truck from the leftmost to the rightmost column.

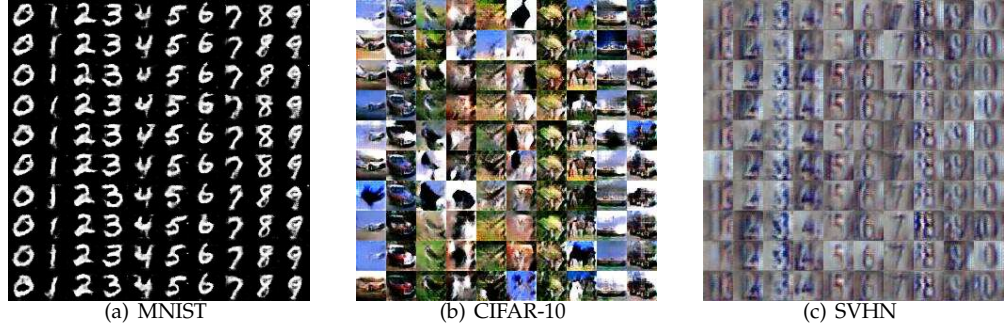


Fig. 4. Illustration of generated images that are similar to one another as they are collapsed to a single mode of the underlying image density on MNIST, CIFAR-10 and SVHN datasets.

pervised learning and data generation that is worth more theoretical and empirical studies in future.

8 CONCLUSION

In this paper, we present a novel Loss-Sensitive GAN (LS-GAN) approach to generate samples from the underlying distributions. The LS-GAN learns a loss function to distinguish generated samples from given examples by imposing the constraint that the loss of a real sample should be sufficiently small by a data dependant margin than that of a generated sample. As the data generator improves, the gap between the losses of real and generated samples will be gradually closed when the generated samples become better and better.

We prove that this approach can generate samples whose data density equals the underlying true data density. Our analysis also suggests that we do not need to assume the model has infinite modeling capacity to obtain this result. Instead we show that a class of generators and loss functions with bounded Lipschitz constants are sufficient to develop the theory for the LS-GAN. A non-parametric solution is derived to characterize the lower and upper bounds of the learned loss functions sought by the LS-GAN.

We also generalize the LS-GAN to a conditional form, yielding the Conditional LS-GAN (CLS-GAN) generating samples under given conditions. Similar theoretical guarantee can be made on the CLS-GAN that ensures the conditional density of its generated samples should be the same as the true conditional data density. Experiment results demonstrate the competitive results on both the image

classification task by using the learned loss function, and the image generation task to produce images of given classes.

APPENDIX A

PROOF OF LEMMA 1

To prove Lemma 1, we need the following lemma.

Lemma 3. *For two probability densities $p(\mathbf{x})$ and $q(\mathbf{x})$, if $p(\mathbf{x}) \geq \eta q(\mathbf{x})$ almost everywhere, we have*

$$\int_{\mathbf{x}} |p(\mathbf{x}) - q(\mathbf{x})| d\mathbf{x} \leq \frac{2(1-\eta)}{\eta}$$

for $\eta \in (0, 1]$.

Proof. We have the following equalities and inequalities:

$$\begin{aligned}
 & \int_{\mathbf{x}} |p(\mathbf{x}) - q(\mathbf{x})| d\mathbf{x} \\
 &= \int_{\mathbf{x}} \mathbb{1}_{[p(\mathbf{x}) \geq q(\mathbf{x})]} (p(\mathbf{x}) - q(\mathbf{x})) d\mathbf{x} \\
 &+ \int_{\mathbf{x}} \mathbb{1}_{[p(\mathbf{x}) < q(\mathbf{x})]} (q(\mathbf{x}) - p(\mathbf{x})) d\mathbf{x} \\
 &= \int_{\mathbf{x}} (1 - \mathbb{1}_{[p(\mathbf{x}) < q(\mathbf{x})]}) (p(\mathbf{x}) - q(\mathbf{x})) d\mathbf{x} \\
 &+ \int_{\mathbf{x}} \mathbb{1}_{[p(\mathbf{x}) < q(\mathbf{x})]} (q(\mathbf{x}) - p(\mathbf{x})) d\mathbf{x} \\
 &= 2 \int_{\mathbf{x}} \mathbb{1}_{[p(\mathbf{x}) < q(\mathbf{x})]} (q(\mathbf{x}) - p(\mathbf{x})) d\mathbf{x} \\
 &\leq 2 \left(\frac{1}{\eta} - 1 \right) \int_{\mathbf{x}} \mathbb{1}_{[p(\mathbf{x}) < q(\mathbf{x})]} p(\mathbf{x}) d\mathbf{x} \\
 &\leq \frac{2(1-\eta)}{\eta}
 \end{aligned} \tag{16}$$

This completes the proof. \square

Now we can prove Lemma 1.

Proof. Suppose (θ^*, ϕ^*) is a Nash equilibrium for the problem (6) and (7).

Then, on one hand, we have

$$\begin{aligned} S(\theta^*, \phi^*) &\geq \mathbb{E}_{\mathbf{x} \sim P_{data}(\mathbf{x})} L_{\theta^*}(\mathbf{x}) \\ &+ \lambda \mathbb{E}_{\substack{\mathbf{x} \sim P_{data}(\mathbf{x}) \\ \mathbf{z}_G \sim P_{G^*}(\mathbf{z}_G)}} (\Delta(\mathbf{x}, \mathbf{z}_G) + L_{\theta^*}(\mathbf{x}) - L_{\theta^*}(\mathbf{z}_G)) \\ &= \int_{\mathbf{x}} P_{data}(\mathbf{x}) L_{\theta^*}(\mathbf{x}) d\mathbf{x} + \lambda \mathbb{E}_{\substack{\mathbf{x} \sim P_{data}(\mathbf{x}) \\ \mathbf{z}_G \sim P_{G^*}(\mathbf{z}_G)}} \Delta(\mathbf{x}, \mathbf{z}_G) \\ &+ \lambda \int_{\mathbf{x}} P_{data}(\mathbf{x}) L_{\theta^*}(\mathbf{x}) d\mathbf{x} - \lambda \int_{\mathbf{z}_G} P_{G^*}(\mathbf{z}_G) L_{\theta^*}(\mathbf{z}_G) d\mathbf{z}_G \\ &= \int_{\mathbf{x}} ((1 + \lambda) P_{data}(\mathbf{x}) - \lambda P_{G^*}(\mathbf{x})) L_{\theta^*}(\mathbf{x}) d\mathbf{x} \\ &+ \lambda \mathbb{E}_{\substack{\mathbf{x} \sim P_{data}(\mathbf{x}) \\ \mathbf{z}_G \sim P_{G^*}(\mathbf{z}_G)}} \Delta(\mathbf{x}, \mathbf{z}_G) \end{aligned} \quad (17)$$

where the first inequality follows from $(a)_+ \geq a$.

We also have $T(\theta^*, \phi^*) \leq T(\theta^*, \phi)$ for any G_ϕ as ϕ minimizes $T(\theta^*, \phi)$. By replacing $P_G(\mathbf{x})$ in $T(\theta^*, \phi)$ with $P_{data}(\mathbf{x})$, we obtain

$$\int_{\mathbf{x}} L_{\theta^*}(\mathbf{x}) P_{G^*}(\mathbf{x}) d\mathbf{x} \leq \int_{\mathbf{x}} L_{\theta^*}(\mathbf{x}) P_{data}(\mathbf{x}) d\mathbf{x}.$$

Applying this inequality into (17) leads to

$$\begin{aligned} S(\theta^*, \phi^*) &\geq \int_{\mathbf{x}} P_{data}(\mathbf{x}) L_{\theta^*}(\mathbf{x}) d\mathbf{x} + \lambda \mathbb{E}_{\substack{\mathbf{x} \sim P_{data}(\mathbf{x}) \\ \mathbf{z}_G \sim P_{G^*}(\mathbf{z}_G)}} \Delta(\mathbf{x}, \mathbf{z}_G) \\ &\geq \lambda \mathbb{E}_{\substack{\mathbf{x} \sim P_{data}(\mathbf{x}) \\ \mathbf{z}_G \sim P_{G^*}(\mathbf{z}_G)}} \Delta(\mathbf{x}, \mathbf{z}_G) \end{aligned} \quad (18)$$

where the last inequality follows as $L_\theta(\mathbf{x})$ is lower bounded by zero.

On the other hand, consider a particular loss function

$$L_\theta(\mathbf{x}) = \alpha(-(1 + \lambda) P_{data}(\mathbf{x}) + \lambda P_{G^*}(\mathbf{x}))_+ \quad (19)$$

When α is a sufficiently small positive coefficient, $L_\theta(\mathbf{x})$ is a nonexpansive function (i.e., a function with Lipschitz constant no larger than 1.). This follows from the assumption that P_{data} and P_G are Lipschitz. In this case, we have

$$\Delta(\mathbf{x}, \mathbf{z}_G) + L_\theta(\mathbf{x}) - L_\theta(\mathbf{z}_G) \geq 0 \quad (20)$$

Thus, one can show that

$$\begin{aligned} S(\theta, \phi^*) &= \int_{\mathbf{x}} ((1 + \lambda) P_{data}(\mathbf{x}) - \lambda P_{G^*}(\mathbf{x})) L_\theta(\mathbf{x}) d\mathbf{x} \\ &+ \lambda \mathbb{E}_{\substack{\mathbf{x} \sim P_{data}(\mathbf{x}) \\ \mathbf{z}_G \sim P_{G^*}(\mathbf{z}_G)}} \Delta(\mathbf{x}, \mathbf{z}_G) \\ &= -\alpha \int_{\mathbf{x}} (-(1 + \lambda) P_{data}(\mathbf{x}) + \lambda P_{G^*}(\mathbf{x}))_+^2 d\mathbf{x} \\ &+ \lambda \mathbb{E}_{\substack{\mathbf{x} \sim P_{data}(\mathbf{x}) \\ \mathbf{z}_G \sim P_{G^*}(\mathbf{z}_G)}} \Delta(\mathbf{x}, \mathbf{z}_G) \end{aligned}$$

where the first equality uses Eq. (20), and the second equality is obtained by substituting $L_\theta(\mathbf{x})$ in Eq. (19) into the equation.

Assuming that $(1 + \lambda) P_{data}(\mathbf{x}) - \lambda P_{G^*}(\mathbf{x}) < 0$ on a set of nonzero measure, the above equation would be upper bounded by $\lambda \mathbb{E}_{\substack{\mathbf{x} \sim P_{data}(\mathbf{x}) \\ \mathbf{z}_G \sim P_{G^*}(\mathbf{z}_G)}} \Delta(\mathbf{x}, \mathbf{z}_G)$ and we have

$$S(\theta^*, \phi^*) \leq S(\theta, \phi^*) < \lambda \mathbb{E}_{\substack{\mathbf{x} \sim P_{data}(\mathbf{x}) \\ \mathbf{z}_G \sim P_{G^*}(\mathbf{z}_G)}} \Delta(\mathbf{x}, \mathbf{z}_G) \quad (21)$$

This results in a contradiction with Eq. (18). Therefore, we must have

$$P_{data}(\mathbf{x}) \geq \frac{\lambda}{1 + \lambda} P_{G^*}(\mathbf{x}) \quad (22)$$

for almost everywhere. By Lemma 3, we have

$$\int_{\mathbf{x}} |P_{data}(\mathbf{x}) - P_{G^*}(\mathbf{x})| d\mathbf{x} \leq \frac{2}{\lambda}$$

Let $\lambda \rightarrow +\infty$, this leads to

$$\int_{\mathbf{x}} |P_{data}(\mathbf{x}) - P_{G^*}(\mathbf{x})| d\mathbf{x} \rightarrow 0$$

This proves that $P_{G^*}(\mathbf{x})$ converges to $P_{data}(\mathbf{x})$ as $\lambda \rightarrow +\infty$. \square

APPENDIX B

PROOF OF THEOREM 2 AND COROLLARY 2

We prove Theorem 2 as follows.

Proof. First, the existence of a minimizer follows from the fact that the functions in \mathcal{F}_κ form a compact set, and the objective function is convex.

To prove the minimizer has the two forms in (10), for each $L_\theta \in \mathcal{F}_\kappa$, let us consider

$$\begin{aligned} \hat{L}_\theta(\mathbf{x}) &= \max_{1 \leq i \leq n+m} \{ (L_\theta(\mathbf{x}^{(i)}) - \kappa \Delta(\mathbf{x}, \mathbf{x}^{(i)}))_+ \}, \\ \tilde{L}_\theta(\mathbf{x}) &= \min_{1 \leq i \leq n+m} \{ L_\theta(\mathbf{x}^{(i)}) + \kappa \Delta(\mathbf{x}, \mathbf{x}^{(i)}) \} \end{aligned}$$

It is not hard to verify that $\hat{L}_\theta(\mathbf{x}^{(i)}) = L_\theta(\mathbf{x}^{(i)})$ and $\tilde{L}_\theta(\mathbf{x}^{(i)}) = L_\theta(\mathbf{x}^{(i)})$ for $1 \leq i \leq n+m$, by noting that L_θ has its Lipschitz constant bounded by κ .

Actually, by Lipschitz continuity, we have $L_\theta(\mathbf{x}^{(i)}) - L_\theta(\mathbf{x}^{(j)}) \leq \kappa \Delta(\mathbf{x}^{(i)}, \mathbf{x}^{(j)})$, and thus

$$L_\theta(\mathbf{x}^{(j)}) - \kappa \Delta(\mathbf{x}^{(i)}, \mathbf{x}^{(j)}) \leq L_\theta(\mathbf{x}^{(i)})$$

Because $L_\theta(\mathbf{x}^{(i)}) \geq 0$ by the assumption (i.e., it is lower bounded by zero), it can be shown that for all j

$$(L_\theta(\mathbf{x}^{(j)}) - \kappa \Delta(\mathbf{x}^{(i)}, \mathbf{x}^{(j)}))_+ \leq L_\theta(\mathbf{x}^{(i)}).$$

Hence, by the definition of $\hat{L}_\theta(\mathbf{x})$ and taking the maximum over j on the left hand side, we have

$$\hat{L}_\theta(\mathbf{x}^{(i)}) \leq L_\theta(\mathbf{x}^{(i)})$$

On the other hand, we have

$$\hat{L}_\theta(\mathbf{x}^{(i)}) \geq L_\theta(\mathbf{x}^{(i)})$$

because $\hat{L}_\theta(\mathbf{x}) \geq (L_\theta(\mathbf{x}^{(i)}) - \kappa \Delta(\mathbf{x}, \mathbf{x}^{(i)}))_+$ for any \mathbf{x} , and it is true in particular for $\mathbf{x} = \mathbf{x}^{(i)}$. This shows $\hat{L}_\theta(\mathbf{x}^{(i)}) = L_\theta(\mathbf{x}^{(i)})$. Likewise, we can prove that $\tilde{L}_\theta(\mathbf{x}^{(i)}) = L_\theta(\mathbf{x}^{(i)})$.

Similarly, one can prove $\tilde{L}_\theta(\mathbf{x}^{(i)}) = L_\theta(\mathbf{x}^{(i)})$. To show this, we have

$$L_\theta(\mathbf{x}^{(j)}) + \kappa \Delta(\mathbf{x}^{(i)}, \mathbf{x}^{(j)}) \geq L_\theta(\mathbf{x}^{(i)})$$

by the Lipschitz continuity of L_θ . By taking the minimum over j , we have

$$\tilde{L}_\theta(\mathbf{x}^{(i)}) \geq L_\theta(\mathbf{x}^{(i)}).$$

On the other hand, we have $\tilde{L}_\theta(\mathbf{x}^{(i)}) \leq L_\theta(\mathbf{x}^{(i)})$ by the definition of $\tilde{L}_\theta(\mathbf{x}^{(i)})$. Combining these two inequalities shows that $\tilde{L}_\theta(\mathbf{x}^{(i)}) = L_\theta(\mathbf{x}^{(i)})$.

Now we can prove for any function $L_\theta \in \mathcal{F}_\kappa$, there exist \hat{L}_θ and \tilde{L}_θ both of which attain the same value of $S_{n,m}$ as L_θ , since $S_{n,m}$ only depends on the values of L_θ on the data points $\{\mathbf{x}^{(i)}\}$. In particular, this shows that any global minimum in \mathcal{F}_κ of $S_{n,m}$ can also be attained by the corresponding functions of the form (10). By setting $l_i^* = \hat{L}_{\theta^*}(\mathbf{x}^{(i)}) = \tilde{L}_{\theta^*}(\mathbf{x}^{(i)})$ for $i = 1, \dots, n+m$, this completes the proof. \square

Finally, we prove Corollary 2 that bounds L_θ with $\hat{L}_\theta(\mathbf{x})$ and $\tilde{L}_\theta(\mathbf{x})$ constructed above.

Proof. By the Lipschitz continuity, we have

$$L_\theta(\mathbf{x}^{(i)}) - \kappa \Delta(\mathbf{x}, \mathbf{x}^{(i)}) \leq L_\theta(\mathbf{x})$$

Since $L_\theta(\mathbf{x}) \geq 0$, it follows that

$$(L_\theta(\mathbf{x}^{(i)}) - \kappa \Delta(\mathbf{x}, \mathbf{x}^{(i)}))_+ \leq L_\theta(\mathbf{x})$$

Taking the maximum over i on the left hand side, we obtain

$$\hat{L}_\theta(\mathbf{x}) \leq L_\theta(\mathbf{x})$$

This proves the lower bound.

Similarly, we have by Lipschitz continuity

$$L_\theta(\mathbf{x}) \leq \kappa \Delta(\mathbf{x}, \mathbf{x}^{(i)}) + L_\theta(\mathbf{x}^{(i)})$$

which, by taking the minimum over i on the left hand side, leads to

$$\tilde{L}_\theta(\mathbf{x}) \leq L_\theta(\mathbf{x})$$

This shows the upper bound. \square

REFERENCES

- [1] I. Goodfellow, J. Pouget-Abadie, M. Mirza, B. Xu, D. Warde-Farley, S. Ozair, A. Courville, and Y. Bengio, "Generative adversarial nets," in *Advances in Neural Information Processing Systems*, 2014, pp. 2672–2680.
- [2] A. Radford, L. Metz, and S. Chintala, "Unsupervised representation learning with deep convolutional generative adversarial networks," *arXiv preprint arXiv:1511.06434*, 2015.
- [3] T. Salimans, I. Goodfellow, W. Zaremba, V. Cheung, A. Radford, and X. Chen, "Improved techniques for training gans," in *Advances in Neural Information Processing Systems*, 2016, pp. 2226–2234.
- [4] D. H. Wolpert, "The lack of a priori distinctions between learning algorithms," *Neural computation*, vol. 8, no. 7, pp. 1341–1390, 1996.
- [5] E. L. Denton, S. Chintala, R. Fergus *et al.*, "Deep generative image models using a laplacian pyramid of adversarial networks," in *Advances in neural information processing systems*, 2015, pp. 1486–1494.
- [6] D. J. Im, C. D. Kim, H. Jiang, and R. Memisevic, "Generating images with recurrent adversarial networks," *arXiv preprint arXiv:1602.05110*, 2016.
- [7] J. Zhao, M. Mathieu, and Y. LeCun, "Energy-based generative adversarial network," *arXiv preprint arXiv:1609.03126*, 2016.
- [8] S. Nowozin, B. Cseke, and R. Tomioka, "f-gan: Training generative neural samplers using variational divergence minimization," *arXiv preprint arXiv:1606.00709*, 2016.
- [9] X. Chen, Y. Duan, R. Houthooft, J. Schulman, I. Sutskever, and P. Abbeel, "Infogan: Interpretable representation learning by information maximizing generative adversarial nets," in *Advances in Neural Information Processing Systems*, 2016, pp. 2172–2180.
- [10] L. A. Gatys, A. S. Ecker, and M. Bethge, "A neural algorithm of artistic style," *arXiv preprint arXiv:1508.06576*, 2015.
- [11] A. Dosovitskiy, J. Tobias Springenberg, and T. Brox, "Learning to generate chairs with convolutional neural networks," in *Proceedings of the IEEE Conference on Computer Vision and Pattern Recognition*, 2015, pp. 1538–1546.
- [12] K. Gregor, I. Danihelka, A. Graves, D. J. Rezende, and D. Wierstra, "Draw: A recurrent neural network for image generation," *arXiv preprint arXiv:1502.04623*, 2015.
- [13] D. P. Kingma, S. Mohamed, D. J. Rezende, and M. Welling, "Semi-supervised learning with deep generative models," in *Advances in Neural Information Processing Systems*, 2014, pp. 3581–3589.
- [14] D. P. Kingma and M. Welling, "Auto-encoding variational bayes," *arXiv preprint arXiv:1312.6114*, 2013.
- [15] A. Rasmus, M. Berglund, M. Honkala, H. Valpola, and T. Raiko, "Semi-supervised learning with ladder networks," in *Advances in Neural Information Processing Systems*, 2015, pp. 3546–3554.
- [16] H. Valpola, "From neural pca to deep unsupervised learning," *Adv. in Independent Component Analysis and Learning Machines*, pp. 143–171, 2015.
- [17] J. T. Springenberg, "Unsupervised and semi-supervised learning with categorical generative adversarial networks," *arXiv preprint arXiv:1511.06390*, 2015.
- [18] K. C. Border, *Fixed point theorems with applications to economics and game theory*. Cambridge university press, 1989.
- [19] D. Carando, R. Fraiman, and P. Groisman, "Nonparametric likelihood based estimation for a multivariate lipschitz density," *Journal of Multivariate Analysis*, vol. 100, no. 5, pp. 981–992, 2009.
- [20] D. Kingma and J. Ba, "Adam: A method for stochastic optimization," *arXiv preprint arXiv:1412.6980*, 2014.
- [21] A. Coates and A. Y. Ng, "Selecting receptive fields in deep networks," in *Advances in Neural Information Processing Systems*, 2011, pp. 2528–2536.
- [22] K. Y. Hui, "Direct modeling of complex invariances for visual object features," in *International Conference on Machine Learning*, 2013, pp. 352–360.
- [23] A. Dosovitskiy, P. Fischer, J. T. Springenberg, M. Riedmiller, and T. Brox, "Discriminative unsupervised feature learning with exemplar convolutional neural networks."
- [24] M. Mirza and S. Osindero, "Conditional generative adversarial nets," *arXiv preprint arXiv:1411.1784*, 2014.
- [25] A. Krizhevsky, "Learning multiple layers of features from tiny images," 2009.
- [26] Y. Netzer, T. Wang, A. Coates, A. Bissacco, B. Wu, and A. Y. Ng, "Reading digits in natural images with unsupervised feature learning," 2011.
- [27] J. Zhao, M. Mathieu, R. Goroshin, and Y. LeCun, "Stacked what-where auto-encoders," *arXiv preprint arXiv:1506.02351*, 2015.
- [28] T. Miyato, S.-i. Maeda, M. Koyama, K. Nakae, and S. Ishii, "Distributional smoothing by virtual adversarial examples," *arXiv preprint arXiv:1507.00677*, 2015.
- [29] L. Maaløe, C. K. Sønderby, S. K. Sønderby, and O. Winther, "Auxiliary deep generative models," *arXiv preprint arXiv:1602.05473*, 2016.